2022 IEEE 61st Conference on Decision and Control (CDC)
December 6-9, 2022. Cancún, Mexico

Optimal Control of Active Drifter Systems

Eric Gaskell and Xiaobo Tan

Abstract— **Drifters are energy-efficient sampling platforms for waterways and other water bodies with pronounced flows. The motion of passive drifters is determined by the underlying flow and thus limited. To overcome this limitation and enhance maneuverability, we consider an active drifter, which has a variable control surface for modulating the hydrodynamic drag force, and a thruster for propulsion or braking. In order to maintain the active drifter as an energy-efficient platform, the use of the thruster must be sparing and carefully considered. In this paper we present an optimal control problem for a one-degree-of-freedom active drifter system, where the cost function aims to balance the objectives of shortest time and minimal thruster use. Despite the complex, realistic nonlinear dynamics of the active drifter, an analytical solution to the optimal control is found by exploiting PMP. In particular, for a given desired final state, each candidate optimal control solution is propagated backward in time, to compute the points in the state space where the optimal control switches; such points are parameterized by the co-state variables, linked implicitly to the system's initial conditions. The proposed approach naturally results in a final-state-dependent partition of the state space, where each region corresponds to a given optimal control value. A feedback control law is readily derived from the aforementioned map. The efficacy of the proposed approach is supported with a numerical example, where the trade-off between time-optimality and fuel-efficiency is illustrated.**

I. Introduction

Before the advent of modern robotic platforms, engineers sought to measure waterway quality with stationary analyzers [1], [2]. Mobile platforms offer the advantage that they may sample measurements at different points in a waterway, reducing the number of sensors required. Drifters have been a popular choice of measurement platform for collecting data in waterways, because they take very little energy to operate. Examples of measurements taken from drifter platforms include iron fertilization, Lagrangian current measurements, light fluxes, and photochemical processes in seawater [3]–[6]. Drifters may also collect meteorological data, communicate with other marine measurement platforms, or listen for the presence of acoustically tagged fish.

More sophisticated drifter systems such as Argo floats are able to make measurements at different depths in the water column [7]. Data collected from Argo floats have been used to predict rainfall and infer monsoon signals in the Bay of Bengal [8]. Expanding the capabilities of marine data collection networks can potentially save thousands of lives from meteorological disasters. Participants in the Argo program are also interested in minimizing energy consumption of the measurement platforms. Work by Riser *et al.* allows for low-power sensors on Argo floats that can potentially operate for years [8]. Like other passive drifters, the floats used in the Argo program will drift wherever the current takes them, which poses a significant limitation in the maneuverability and thus the capability of these platforms.

In our prior work [9], [10] we proposed a steerable drifter that could modulate the hydrodynamic forces acting on its rudders. By changing the angles of the rudders, steerable drifters are able to exert some degree of control over their motion by modulating the effective drag force on the platform. However, as the drifter's velocity approaches that of the ambient flow, the latitude of such control is diminished. Therefore in this work we consider an active drifter, which, in addition to being able to modulate the hydrodynamic drag force via its control surfaces (such as rudders), has a thruster to produce propulsion and braking. The thruster force will not only allow the drifter to directly change its velocity, but also produce the velocity differential with respect to the ambient flow that is needed for drag-based maneuvers. In order to maintain active drifters as a low-energy platform, however, the use of the thruster must be sparing and planned carefully. In this paper an optimal control problem for a one-degree-of-freedom (DoF) active drifter system is studied, where the cost function aims to balance the objectives of shortest time and minimal thruster use. We note that the considered one DoF setting is not particularly restrictive, because drifter systems in rivers and in large lake or ocean currents move primarily with the direction of the ambient flow; for active drifters, control along this axis is one-dimensional.

We note that optimal control has been studied in various contexts and numerous methods have been developed in the literature. In particular, Pontryagin's Minimum Principle (PMP) [11] has been applied to a wide variety of control problems from loop-shaping to solving the Nash differential games [12], [13]. While a powerful result, it can be difficult to solve the system of equations presented by PMP to find the optimal feedforward control. Numerical methods such as the shooting approach can sometimes be used [14] [15]. When these equations cannot be easily solved, methods such as that discussed by Guo *et al.* [16] could be employed to solve the Hamilton-Jacobi-Bellman (HJB) equation. Even for cases in which the optimal control law is known, singularities in the solution could force designers to resort to methods such as that used by Rodrigo and Patiño [17]. In general, it is rare to be able to obtain analytical optimal control solutions for systems with nonlinear dynamics.

Eric M. Gaskell and Xiaobo Tan are with the Department of Electrical and Computer Engineering, Michigan State University, East Lansing, MI 48824. Email: gaskelle@msu.edu (E.M.G.), xbtan@egr.msu.edu (X.T.)

This work was supported by the National Science Foundation (IIS 1848945 and ECCS 2030556) and the Great Lakes Fishery Commission (2022_TAN_441020).

In this work, despite the complex, realistic nonlinear dynamics for the active drifter system, a novel approach is proposed to derive an analytical solution to the optimal control problem by exploiting PMP. In particular, for a given desired final state, each candidate optimal control solution is propagated backward in time, to compute the points in the state space where the optimal control switches. For a chosen final state (drifter position and velocity), bounds on state space regions corresponding to different optimal control values are determined, parameterized by one of the costate variables. From these boundaries, final-state-dependent feedback control maps are synthesized.

By using these maps, the optimal control for reaching a chosen final state can be found with state feedback rather than by solving a system of differential equations for the state and costate. The efficacy of the proposed approach is supported with a numerical example, where the aforementioned feedback control law is shown to drive the system to its desired final configuration even in the presence of ambient disturbances. Furthermore, the derived feedback control law has explicit dependence on the parameter λ characterizing the trade-off between time-optimality and fuel-efficiency, and the numerical example confirms the desired trade-off behavior as λ is varied.

The remainder of the paper is organized as follows. In Section II the model for the active drifter and the formulation of the optimal control problem are presented. In Section III the approach to the derivation of the analytical optimal control solution is elaborated. The numerical example is discussed in Section IV, followed by some concluding remarks in Section V.

II. Problem Formulation

The active drifter system considered in this work is assumed to be capable of modulating its drag force as well as producing propulsion with a thruster. Drifters primarily move with the current, making control along this dimension essential for active drifter systems. Therefore, we consider the one degree-of-freedom setup. The dynamic model for the active drifter is similar to those proposed by Gaskell and Tan [9], [10], with the key differences being that it includes the effect of a thruster and is focused on the dynamics along the flow direction. In particular, the system dynamics takes the following form:

$$\dot{x} = \begin{bmatrix} \dot{x_1} \\ \dot{x_2} \end{bmatrix} = \begin{bmatrix} x_2 \\ -a(x_2 - \sigma)|x_2 - \sigma|u_1 + bu_2 \end{bmatrix} \tag{1}$$

where $x_1 \in \mathbb{R}, x_2 \in \mathbb{R}$ are the system states that represent the drifter's position and velocity, respectively, σ is the constant ambient flow velocity, $a > 0$ is a constant associated with the drag force, $b > 0$ is a coefficient related to the thruster force, and u_1, u_2 are the applied controls, which modulate the strengths of the drag force and thruster force, respectively. Note that the drag force is proportional to the square of the drifter velocity $x_2 - \sigma$ relative to the flow and acts in the opposite direction of the relative velocity. The control inputs are subject to the following constraints: $u_1 \in \{c, 1\}, u_2 \in \{-1, 0, 1\}$, where $c \in (0, 1]$. The parameter c represents the ratio of the minimum drag force to the maximum drag force achievable through modulation.

Active drifters modulate their drag by rotating one or more rudders, but do not use much energy to hold rudders still. Based on practical considerations, it is assumed that modulating the drag on a drifter will accordingly not require much energy, but that activating the thruster will. A cost functional L is thus defined as:

$$L(u(t)) = \lambda + (1 - \lambda)|u_2(t)| \tag{2}$$

where $\lambda \in (0, 1)$ represents the trade-off between the two objectives of shortest time and minimal fuel, respectively. A value of λ close to 1 will incur a high penalty for time taken and a low penalty for fuel use. Inversely, a value of λ close to 0 will incur a low penalty for time taken and a high penalty for fuel use.

Given an initial state of the system $x(t_0) = (x_{0,1}, x_{0,2})^T$ and a final state $x_f = x(t_f) = (x_{f,1}, x_{f,2})^T$, we aim to find the control $u = (u_1, u_2)^T$ that minimizes the cost

$$J(x(t_0), u(\cdot)) = \int_{t_0}^{t_f} L(u(t))\mathrm{d}t \tag{3}$$

where t_f is the final time where $x(t_f) = (x_{f,1}, x_{f,2})^T$. Controlling such a system to a desired final state x_f while minimizing the integral of a cost functional normally requires solving a system of differential equations for the state and the costate. With the nonlinear dynamics, solving these adjoint different equations typically has to resort to approximating numerical methods, and the resulting solution is often a time-parametrized feedforward control function, which is not robust to system uncertainties or external disturbances.

This work seeks to map the optimal control inputs to the state space. This map can then be used to select the optimal control for an arbitrary state x through state feedback. Such a feedback control approach will not only be simpler to calculate and implement, but also be more robust (than the feedforward solution).

III. Optimal Control by Pontryagin's Minimum Principle

This section presents our approach to the analytical computation of the PMP-based optimal control solution for the active drifter system. First, necessary conditions for optimal control are considered, and the approach to the derivation of the solution is presented.

A. Necessary Conditions for Optimal Control

The Minimum Principle requires several necessary conditions for a control to be optimal [11]. Solutions to the optimal control problem may be found through examination of these necessary conditions:

- The applied control needs to minimize the system Hamiltonian H with respect to the control input;
- The evolution of the costate p satisfies $\dot{p} = -\nabla_x H$, where $\nabla_x H$ denotes the gradient of H with respect to the state x;

- The Hamiltonian is uniformly equal to 0 over the entire trajectory, i.e, $H \equiv 0$.

First, we examine the potential controls that minimize the Hamiltonian based on the system state and costate. Then, we show that these controls meet the second condition. Finally, for a known x_f, we find piecewise continuous controls satisfying $H \equiv 0$.

In order to facilitate the analysis, define a transformed system state z_2 that represents the relative velocity of the drifter with respect to the ambient flow:

$$z_2 = x_2 - \sigma \tag{4}$$

The dynamics of the transformed system $\bar{x} \triangleq (x_1, z_2)^T$ is given by:

$$\dot{\bar{x}} = \begin{bmatrix} \dot{x_1} \\ \dot{z_2} \end{bmatrix} = \begin{bmatrix} z_2 + \sigma \\ -az_2|z_2|u_1 + bu_2 \end{bmatrix} \tag{5}$$

The Hamiltonian H can then be stated in terms of the transformed system as

$$H = \lambda + (1-\lambda)|u_2| + p_1(z_2+\sigma) + p_2(-az_2|z_2|u_1 + bu_2) \tag{6}$$

where $p \triangleq (p_1, p_2)^T$ is the costate. Eq. (6) can be regrouped according to the control inputs u_1 and u_2:

$$H = \lambda + p_1(z_2+\sigma) + [(1-\lambda)|u_2| + p_2 bu_2] - ap_2 z_2|z_2|u_1 \tag{7}$$

From (7), the control u_1 minimizing the Hamiltonian is

$$u_1^* = \begin{cases} 1, & z_2 p_2 > 0 \\ c, & z_2 p_2 < 0 \\ \in \{0,1\} & z_2 p_2 = 0 \end{cases} \tag{8}$$

Similarly, the optimal control u_2^* that minimizes the Hamiltonian is

$$u_2^* = \begin{cases} 1 & p_2 b < \lambda - 1 \\ -1 & p_2 b > 1 - \lambda \\ 0 & |p_2 b| < 1 - \lambda \\ \in \{-1, 0\} & p_2 b = 1 - \lambda \\ \in \{0, 1\} & p_2 b = \lambda - 1 \end{cases} \tag{9}$$

From (8) and (9), for $z_2 > 0$, if $p_2 < 0$, $u_1^* = c$, and $u_2^* = 0$ or $u_2^* = 1$, but $u_2^* \neq -1$, since $p_2 b < 0 < 1 - \lambda$. Likewise, for $z_2 > 0$, if $p_2 > 0$, $u_1^* = 1$, and $u_2^* = 0$ or $u_2^* = -1$, but $u_2^* \neq 1$, since $p_2 b > 0 > 1 - \lambda$. It can be shown that $p_2 z_2$ cannot remain constantly at 0 for a nontrivial time interval unless $z_2 = 0$ and that $|p_2 b|$ cannot remain at $1 - \lambda$ for a nontrivial time interval unless $z_2 \in \{0, \pm\sqrt{b/(ac)}\}$. To examine these possibilities, state space trajectories of the system are considered. Trajectories in the state space under a constant control are the solutions to (10) under that control

$$\frac{\mathrm{d}x_1}{\mathrm{d}z_2} = \frac{z_2 + \sigma}{-a(z_2)|(z_2)|u_1 + bu_2} \tag{10}$$

By applying a control with $|u_2| = 1, u_1 = c$ and setting $\frac{\mathrm{d}z_2}{\mathrm{d}x_1} = 0$, the asymptotic velocities are

$$z_2 = \pm\sqrt{\frac{b}{ac}} \tag{11}$$

which implies that for velocities between the asymptotic velocities of the system, $|p_2 b|$ cannot remain uniformly at $1 - \lambda$ unless $z_2 = 0$. For the case examined, the trajectories for which $z_2 = 0$ over a nontrivial interval were found to incur a higher cost than simpler but suboptimal control, and therefore they cannot be optimal. For cases not examined, trajectories for which $z_2 = 0$ should be considered.

To illustrate the proposed approach, we present the details of the derivation for one case $\{x_{f,2} > 0, z_{f,2} > 0\}$. Other cases, $\{x_{f,2} > 0, z_{f,2} < 0\}$, $\{x_{f,2} < 0, z_{f,2} < 0\}$, $\{x_{f,2} < 0, z_{f,2} > 0\}$, $\{x_{f,2} = 0\}$, and $\{z_{f,2} = 0\}$ can be solved in a similar manner. As discussed earlier for the case of $z_2 > 0$, there are 4 possible optimal controls in the neighborhood of $\bar{x}_f$ with $z_{f,2} > 0$:

$$u^* \in \left\{ \begin{bmatrix} 1 \\ 0 \end{bmatrix}, \begin{bmatrix} 1 \\ -1 \end{bmatrix}, \begin{bmatrix} c \\ 0 \end{bmatrix}, \begin{bmatrix} c \\ 1 \end{bmatrix} \right\} \tag{12}$$

Our solution will take a back-propagation approach, where we infer the optimal control backward from the final state. By exploring each of the possible controls in (12), we seek to find a complete solution for the entire state space.

The minimizing controls in (12) must also satisfy the condition of $\dot{p} = -\nabla_{\bar{x}} H$ where

$$\nabla_{\bar{x}} H = \begin{bmatrix} 0 \\ p_1 - 2ap_2|z_2|u_1 \end{bmatrix} \tag{13}$$

Note that p_1 must therefore be a constant. A third necessary condition for a control solution to be optimal is that the Hamiltonian must satisfy $H = 0$ for all time t. An expression for p_2 can then be found by applying this condition to (7) and solving for p_2:

$$p_2 = \frac{\lambda + (1-\lambda)|u_2| + p_1(z_2+\sigma)}{az_2|z_2|u_1 - bu_2} \tag{14}$$

Note that for $|z_2| < \sqrt{\frac{b}{ac}}$, the asymptotic speed, and under the controls included in (12), the denominator of p_2 is nonzero. The control input $u = (u_1, u_2)^T$ is piecewise constant, formed from controls included in (12). Because λ, σ, p_1, a, b, and c are also constants, the time derivative of p_2 is then

$$\dot{p}_2 = \frac{1}{(az_2|z_2|u_1 - bu_2)^2} \Big[(az_2|z_2|u_1 - bu_2)(p_1) - (\lambda + (1-\lambda)|u_2| + p_1(z_2+\sigma))(2a|z_2|u_1) \Big] \dot{z}_2 \tag{15}$$

From the system definition in (5),

$$\dot{z}_2 = -(az_2|z_2|u_1 - bu_2) \tag{16}$$

which implies

$$\dot{p}_2 = -p_1 + \frac{\lambda + (1-\lambda)|u_2| + p_1(z_2+\sigma)}{az_2|z_2|u_1 - bu_2}(2a|z_2|u_1) \quad (17)$$

B. Backward Derivation of Optimal Control Switching Points

In order to find the state feedback control from an arbitrary initial state to a fixed final state x_f, the following method is proposed:

1) For each control identified in (12):
   - Assume this to be the optimal final control u_f^* for a family of trajectories terminating at $\bar{x}_f$;
   - Apply (8) and (9) to determine a range of $p_{f,2}$ for this family of trajectories;
   - Solve (14) for p_1 to determine a range of the constant p_1 for this family of trajectories;
   - Solve for any points in the state space where the optimal control changes according to (8) and (9), working backward from the final point $\bar{x}_f$;
   - Treat these points as curves representing the location where the optimal control to reach $\bar{x}_f$ changes, parameterized by p_1.
2) Plot all boundaries found for each family of trajectories in the state space, enclosing regions of different optimal controls.
3) Use this map to derive the state feedback control law.

As an example, we now present the derivation of the solution corresponding to the family of optimal trajectories for which the final optimal control $u_f^* = (1,0)^T$. Solutions corresponding to $u_f^* = \{(1,-1)^T, (c,0)^T, (c,1)^T\}$ may be derived in a similar manner.

From (14), with $u^* = (1,0)^T$, for $z_2 > 0$, p_2 can be expressed as

$$p_2 = \frac{\lambda + p_1(z_2+\sigma)}{az_2^2} \quad (18)$$

In order to satisfy our assumption that this is the optimal final control, we will need $p_2 > 0$ and $|p_2 b| < 1-\lambda$. Applying these constraints and solving for p_1 yields

$$\frac{-\lambda}{z_2+\sigma} < p_1 < \frac{(1-\lambda)az_2^2 - \lambda b}{b(z_2+\sigma)} \quad (19)$$

Note that due to the restrictions placed on $a, b, x_{f,2}, z_{f,2}$ and λ, the right side of (19) will always be greater than the left side. Now we look for any relative velocities $z_{-1,2}$ where the control switches. The first subscript "-1" in z indicates that this would be the first switching point going backward in time. Analogous notations will be applied for other variables in the subsequent derivation. Under the current control with only drag in effect, z_2 cannot change sign, and x_2, z_2 should be more positive as we propagate time backward. From this, we can infer that the control switch will only depend on conditions on p_2. With continuous p_2, the control will either switch at $p_2 = 0$ or $p_2 = \frac{1-\lambda}{b}$. The first condition yields

$$p_{-1,2} = 0 = \frac{\lambda + p_1(z_{-1,2}+\sigma)}{az_{-1,2}^2} \quad (20)$$

(21)

which implies

$$z_{-1,2} = -\frac{\lambda}{p_1} - \sigma \quad (22)$$

Applying the second condition yields

$$p_{-1,2} = \frac{(1-\lambda)}{b} = \frac{\lambda + p_1(z_{-1,2}+\sigma)}{az_{-1,2}^2} \quad (23)$$

(24)

which implies

$$z_{-1,2} = \frac{1}{2a(1-\lambda)}\Big[p_1 b \pm\sqrt{(p_1 b)^2 + 4ab(1-\lambda)(\lambda + p_1\sigma)}\Big] \quad (25)$$

The real solutions in (25), if existing, are either negative (unreachable under this control) or found to satisfy $z_{-1,2} < z_{f,2}$ for all combinations of system parameters examined, indicating they are past the final point. For parameters not examined, this solution may have to be considered. Therefore, the only feasible location of the control switch $\bar{x}_{-1}$ is given by (22). The x_1 coordinate of $\bar{x}_{-1}$ can be found from (10) under this control:

$$-\frac{1}{a}\left[\log(z_2) - \frac{\sigma}{z_2}\right] = x_1 + C_0 \quad (26)$$

where C_0 is a constant. C_0 can be found by evaluating at the known z_f:

$$x_{-1,1} = \frac{1}{a}\left[\log\left(\frac{z_{f,2}}{z_{-1,2}}\right) + \sigma\left[\frac{1}{z_{-1,2}} - \frac{1}{z_{f,2}}\right]\right] + x_{f,1} \quad (27)$$

At $\bar{x}_{-1}$, $p_2 = 0$. From (8), at $p_2 = 0$ the control switches from $u = (c,0)^T$ to $u = (1,0)^T$, which the system follows until reaching $\bar{x}_f$.

Using a similar process to propagate backward in time, the optimal control is found to switch at a point $\bar{x}_{-2}$. Here the control switches from $u = (c,1)^T$ to $u = (c,0)^T$, which the system follows until reaching $\bar{x}_{-1}$. In particular, one can derive, at $\bar{x}_{-2}$,

$$z_{-2,2} = \frac{-1}{2(1-\lambda)ac}\Big[p_1 b + \sqrt{(p_1 b)^2 - 4(\lambda + p_1\sigma)(1-\lambda)abc}\Big] \quad (28)$$

and $x_{-2,1}$ can be found from (10) under the control $u = (c,0)^T$:

$$x_{-2,1} = \frac{1}{ac}\left[\log\left(\frac{z_{-1,2}}{z_{-2,2}}\right) + \sigma\left(\frac{1}{z_{-2,2}} - \frac{1}{z_{-1,2}}\right)\right] + x_{-1,1} \tag{29}$$

The next point where the optimal control switches, $\bar{x}_{-3}$, occurs where the trajectories in this family cross $z_2 = 0$. Here the control switches from $u = (1,1)^T$ to $u = (c,1)^T$, which the system follows until reaching $\bar{x}_{-2}$.

$$z_{-3,2} = 0 \tag{30}$$

from which $x_{-3,1}$ can be expressed as

$$x_{-3,1} = -\frac{1}{2ac}\log\left[\frac{b}{b - acz_{-2,2}^2}\right] - \frac{\sigma \tanh^{-1}\left(\sqrt{\frac{ac}{b}}z_{-2,2}\right)}{\sqrt{abc}} + x_{-2,1} \tag{31}$$

For this family of trajectories, one final point $\bar{x}_{-4}$ is identified where the optimal control changes from $u = (1,0)^T$ to $u = (1,1)^T$, which the system follows until reaching $\bar{x}_{-3}$. By applying the condition $p_2 b = \lambda - 1$,

$$z_{-4,2} = \frac{1}{2a(1-\lambda)}\Big[p_1 b - \sqrt{(p_1 b)^2 + 4ab(1-\lambda)(\lambda + p_1\sigma)}\Big] \tag{32}$$

from which $x_{-4,1}$ can be expressed as

$$x_{-4,1} = \frac{\sigma}{\sqrt{ab}}\arctan\left(z_{j2}\sqrt{a/b}\right) - \frac{1}{2a}\log\left(\frac{b}{az_{-4,2}^2 + b}\right) + x_{-3,1} \tag{33}$$

Solutions corresponding to further control switches are attempted, but one can show there are no more real, feasible solutions. Thus, $\bar{x}_{-4}$ is the state space location for the final control switch. This process is repeated for each family of trajectories corresponding to different final optimal controls until no further locations can be identified where the optimal control changes.

C. Feedback Control Maps

Control switching points as calculated above can be thought of as curves in the state space parameterized by p_1 over the range of p_1 for their respective families of trajectories. By plotting these curves in the state space, regions may be found over which the optimal control to reach x_f is the same. Where necessary, these regions are closed with trajectories formed by constant control such that any point in the state-space belongs to exactly one region.

For example, all trajectories for which $u_f^* = (c,1)^T$ cross $z_2 = 0$ at the same point. Between this point and x_f, a boundary was formed from the trajectory under this control input. This boundary separates regions for which $u^* = (c,1)^T$ from regions for which $u^* = (1,-1)^T$. From the continuity of the costate, such a switch cannot occur. However, examination of possible optimal trajectories suggests that this trajectory forms the boundary for which feasible trajectories from x_i (the initial state) to x_f exist for each control input.

As an example, for $a = 1$, $b = 1$, $c = 0.5$, $\sigma = 0.3$, $x_f = (0, 0.5)^T$, maps of the optimal control generated for $\lambda = \{0.2, 0.5, 0.8\}$, are shown in Figs. 1 - 3.

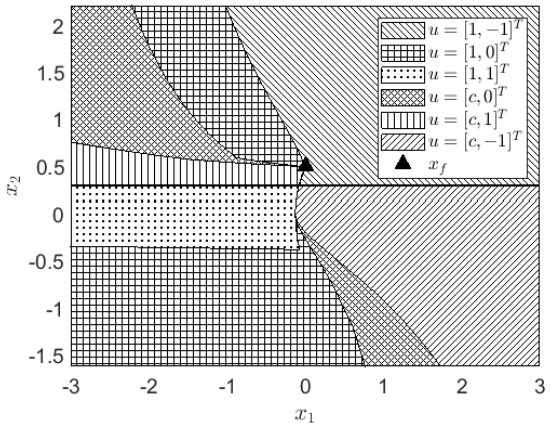

Fig. 1. Feedback control map showing the optimal control to reach x_f for $\lambda = 0.2$.

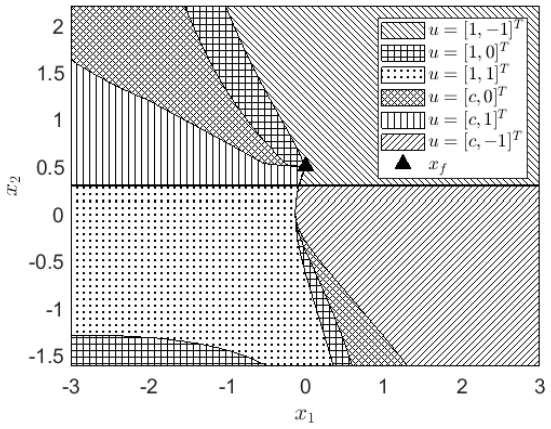

Fig. 2. Feedback control map showing the optimal control to reach x_f for $\lambda = 0.5$.

In Fig. 1, for which $\lambda = 0.2$, there are large regions for which $u_2 = 0$. This is because there is a small penalty associated with time, but a large penalty for applying force with the thruster. These regions shrink as λ increases to $\lambda = 0.5$ in Fig. 2, and shrink further as λ increases to $\lambda = 0.8$ in Fig. 3.

IV. Simulation Results

For an initial condition $x_i = (-2, 0.1)^T$ and the required final state $x_f = (0, 0.5)^T$, the optimal open-loop control and the corresponding state trajectory are calculated for $\lambda = 0.5$. The system trajectory is then calculated under the optimal

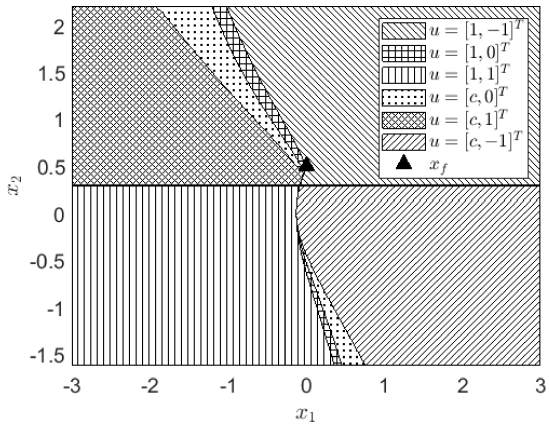

Fig. 3. Feedback control map showing the optimal control to reach x_f for $\lambda = 0.8$.

state feedback controller, derived from the map in Fig. 2. Fig. 4(a) shows the corresponding state trajectories under both controls, where one can see they overlap with each other. This agreement shows that, in the absence of any disturbance, the feedback control produces consistent results as the optimal open-loop control calculated with PMP.

We further simulate the controlled drifter behavior when the system is subject to external disturbances. An additive white Gaussian noise (AWGN) term w, representing a disturbance force, is added to the model. The optimal feedforward control and the optimal feedback control, respectively, are then applied to the model with disturbance, and the corresponding trajectories are shown in Fig. 4(b). It can be seen that the system fails to reach the required final state under the pre-calculated optimal feedforward control, while the feedback control is able to take the drifter to the desired final state despite the presence of the disturbances.

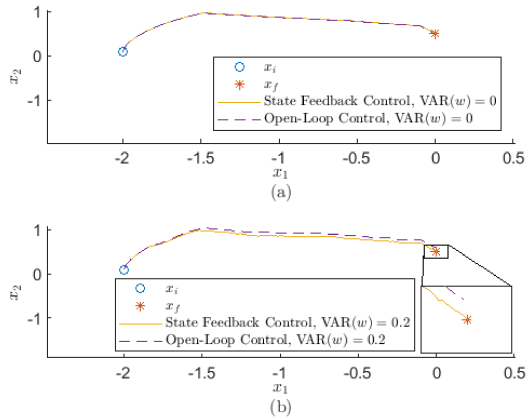

Fig. 4. (a) Simulated trajectories under the optimal feedforward control and the optimal feedback control, in the absence of disturbance; (b) simulated trajectories under the optimal feedforward control and the optimal feedback control, in the presence of the disturbance w with variance of 0.2.

Finally, the optimal feedback control is simulated without disturbance for the same x_i but different values for the trade-off parameter $\lambda = \{0.2, 0.5, 0.8\}$. The resulting control inputs are shown in Fig. 5, while the trajectories corresponding to these controls are shown in Fig. 6. From Figs. 5 and 6, the effect of λ on the optimal control can be seen. As the penalty for the thruster use is increased relative to the penalty for time taken, the thruster is activated for shorter intervals, the active drifter remains in drift for longer periods, and it takes a longer time to reach x_f.

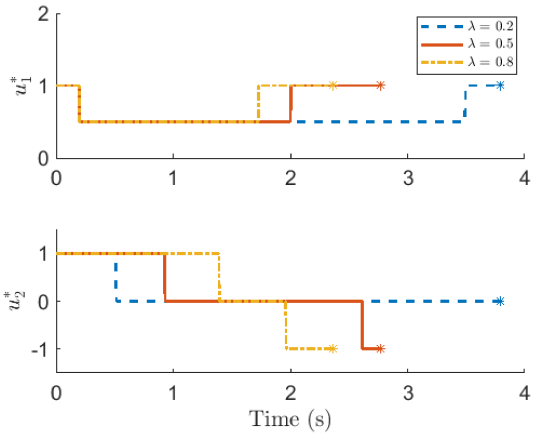

Fig. 5. Comparison of the optimal state feedback control for $\lambda = \{0.2, 0.5, 0.8\}$. Final optimal controls are marked with asterisks.

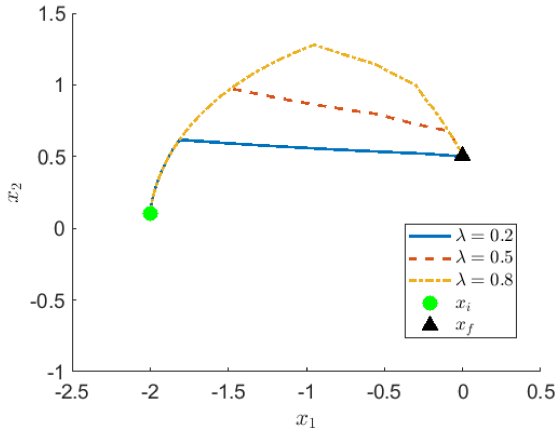

Fig. 6. Comparison of the state trajectories under optimal state feedback control for $\lambda = \{0.2, 0.5, 0.8\}$

V. Conclusion

Active drifters are promising energy-efficient sampling platforms for sampling in waterways, lakes, and oceans. In this work we examined the optimal control problem for one-degree-of-freedom active drifters with nonlinear dynamics. The proposed approach was shown to generate PMP-based analytical solutions to the optimal control problem. Furthermore, the optimal control was directly mapped to the state space, enabling the derivation of state feedback laws. The effect of varying λ was examined on the optimal control policy. For $\lambda = 0.5$, the system was simulated under

disturbance, and the resulting feedback control policy was shown to be accurate and robust.

Previous prototypes and models of steerable drifters established in [9] and [10] modulate their drag with a pair of rudders. Through symmetric operation of rudders in such a configuration, drag can effectively be modulated in the longitudinal direction, with the resulting dynamics close to the case of a one-degree-of-freedom system as represented in Eq. (1). We plan to experimentally validate the proposed optimal control approach by implementing it on the physical prototype and evaluating its performance in a river environment. We also plan to compare the performance of this control to paths generated with Rapid Random Trees (RRTs).

ACKNOWLEDGMENT

We thank Drs. Guoming Zhu, Shaunak Bopardikar, and Vaibhav Srivastava for their insightful comments on this work.

REFERENCES

[1] E. J. Cleary, "Development of a robot system," *Journal AWWA*, vol. 50, no. 9, pp. 1219–1222, 1958.

[2] ——, "Robot monitor system for the Ohio Valley," *Journal AWWA*, vol. 54, no. 11, pp. 1347–1352, 1962.

[3] J. K. B. Bishop, R. E. Davis, and J. T. Sherman, "Robotic observations of dust storm enhancement of carbon biomass in the North Pacific," *Science*, vol. 298, no. 5594, pp. 817–821, 2002.

[4] J. K. B. Bishop, T. J. Wood, R. E. Davis, and J. T. Sherman, "Robotic observations of enhanced carbon biomass and export at 55°s during SOFeX," *Science*, vol. 304, no. 5669, pp. 417–420, 2004.

[5] J. Austin and S. Atkinson, "The design and testing of small, low-cost GPS-tracked surface drifters," *Estuaries*, vol. 27, no. 6, pp. 1026–1029, 2004.

[6] D. J. Kieber, B. H. Yocis, and K. Mopper, "Free-floating drifter for photochemical studies in the water column," *Limnology and Oceanography*, vol. 42, no. 8, pp. 1829–1833, 1997.

[7] D. Roemmich, G. C. J. G. C. Johnson, S. Riser, R. D. R. Davis, J. Gilson, W. B. Owens, S. L. Garzoli, C. Schmid, and M. Ignaszewski, "The argo program: Observing the global ocean with profiling floats," *Oceanography*, vol. 22, no. 2, pp. 34–43, 2009.

[8] S. C. Riser, J. Nystuen, and A. Rogers, "Monsoon effects in the bay of bengal inferred from profiling float-based measurements of wind speed and rainfall," *Limnology and Oceanography*, vol. 53, no. 5, pp. 2080–2093, 2008.

[9] E. Gaskell and X. Tan, "Dynamic modeling of a steerable drifter," ser. 2020 ASME Dynamic Systems and Control Conference, vol. Volume 2, 10 2020, v002T28A003. [Online]. Available: https://doi.org/10.1115/DSCC2020-3295

[10] ——, "Adaptive parameter estimation of a steerable drifter," *IFAC-PapersOnLine*, vol. 54, no. 20, pp. 108–113, 2021, modeling, Estimation and Control Conference MECC 2021. [Online]. Available: https://www.sciencedirect.com/science/article/pii/S2405896321022059

[11] L. Bittner, "L. S. Pontryagin, V. G. Boltyanskii, R. V. Gamkrelidze, E. F. Mishechenko, The mathematical theory of optimal processes. VIII + 360 S. New York/London 1962. John Wiley & sons. preis 90/–," *ZAMM - Journal of Applied Mathematics and Mechanics / Zeitschrift für Angewandte Mathematik und Mechanik*, vol. 43, no. 10-11, pp. 514–515, 1963. [Online]. Available: https://onlinelibrary.wiley.com/doi/abs/10.1002/zamm.19630431023

[12] D. Davison, P. Kabamba, and S. Meerkov, "Loop shaping using pontryagin's minimum principle," in *Proceedings of the 1999 American Control Conference (Cat. No. 99CH36251)*, vol. 5, 1999, pp. 3280–3281 vol.5.

[13] G. Xu, B. Zhou, G. Shi, and P. Liao, "Solving nash differential game based on minimum principle and pseudo-spectral method," in *2016 Chinese Control and Decision Conference (CCDC)*, 2016, pp. 173–177.

[14] J. F. Bonnans, "The shooting approach to optimal control problems," *IFAC Proceedings Volumes*, vol. 46, no. 11, pp. 281–292, 2013, 11th IFAC Workshop on Adaptation and Learning in Control and Signal Processing. [Online]. Available: https://www.sciencedirect.com/science/article/pii/S1474667016329597

[15] A. Karbowski, *Shooting Methods to Solve Optimal Control Problems with State and Mixed Control-State Constraints*, 02 2016, pp. 189–205.

[16] B. Z. Guo and B. Sun, "A new algorithm for finding numerical solutions of optimal feedback control law," in *2006 Chinese Control Conference*, 2006, pp. 568–572.

[17] R. H. Rodrigo and D. H. Patiño, "Numerical solution to uncertainties in the finite time optimal control systems design," in *2015 XVI Workshop on Information Processing and Control (RPIC)*, 2015, pp. 1–5.

[18] H. Sussmann and J. Willems, "300 years of optimal control: from the brachystochrone to the maximum principle," *IEEE Control Systems Magazine*, vol. 17, no. 3, pp. 32–44, 1997.

[19] X. Xu and P. Antsaklis, "Optimal control of switched systems based on parameterization of the switching instants," *IEEE Transactions on Automatic Control*, vol. 49, no. 1, pp. 2–16, 2004.

[20] A. Pakniyat and P. E. Caines, "On the hybrid minimum principle: The hamiltonian and adjoint boundary conditions," *IEEE Transactions on Automatic Control*, vol. 66, no. 3, pp. 1246–1253, 2021.

[21] T. Das and R. Mukherjee, "An extension of the minimum principle with application to switched linear systems," in *2006 American Control Conference*, 2006, pp. 2424–2426.

[22] S. Agrawal and T. Veeraklaew, "Optimization of higher-order systems and extensions of minimum principle," in *Proceedings of the 38th IEEE Conference on Decision and Control (Cat. No.99CH36304)*, vol. 1, 1999, pp. 882–887 vol.1.

[23] Y. S. Song and M. R. Arshad, "Robust optimal depth control of hovering autonomous underwater vehicle," in *2017 IEEE 2nd International Conference on Automatic Control and Intelligent Systems (I2CACIS)*, 2017, pp. 191–195.

[24] D. A. Rickert and W. G. Hines, "River quality assessment: Implications of a prototype project," *Science*, vol. 200, no. 4346, pp. 1113–1118, 1978.

[25] I. Kanellakopoulos, M. Krstic, and P. V. Kokotovic, "Interlaced controller-observer design for adaptive nonlinear control," in *1992 American Control Conference*, 1992, pp. 1337–1342.

[26] K. S. Johnson, W. M. Berelson, E. S. Boss, Z. Chase, H. Claustre, S. R. Emerson, N. Gruber, A. Kortzinger, M. J. Perry, and S. C. Riser, "Observing biogeochemical cycles at global scales with profiling floats and gliders: Prospects for a global array," *Oceanography*, vol. 22, no. 3, pp. 216–225, 2009.

[27] J. E. Gaudio, A. M. Annaswamy, J. M. Moreu, M. A. Bolender, and T. E. Gibson, "Accelerated learning with robustness to adversarial regressors," 2020. [Online]. Available: https://arxiv.org/abs/2005.01529